Pure appl. geophys. 163 (2006) 723–744
0033–4553/06/040723–22
DOI 10.1007/s00024-006-0047-9

Pure and Applied Geophysics

Modelling the Mixing Function to Constrain Coseismic Hydrochemical Effects: An Example from the French Pyrénées

Jean-Paul Toutain,[1] Margot Munoz,[1] Jean-Louis Pinaud,[2] Stéphanie Levet,[1] Matthieu Sylvander,[3] Alexis Rigo,[3] and Jocelyne Escalier[1]

Abstract—Groundwater coseismic transient anomalies are evidenced and characterized by modelling the mixing function F characteristic of the groundwater dynamics in the Ogeu (western French Pyrénées) seismic context. Investigations of water-rock interactions at Ogeu indicate that these mineral waters from sedimentary environments result from the mixing of deep waters with evaporitic signature with surficial karstic waters. A 3-year hydrochemical monitoring of Ogeu springwater evidences that using arbitrary thresholds constituted by the mean $\pm$ 1 or 2σ, as often performed in such studies, is not a suitable approach to characterize transient anomalies. Instead, we have used a mixing function F calculated with chemical elements, which display a conservative behavior not controlled by the precipitation of a mineral phase. F is processed with seismic energy release (E_s) and effective rainfalls (R). Linear impulse responses of F to E_s and R have been calculated. Rapid responses (10 days) to rainwater inputs are evidenced, consisting in the recharge of the shallow karstic reservoir by fresh water. Complex impulse response of F to microseismic activity is also evidenced. It consists in a 2-phase hydrologic signal, with an inflow of saline water in the shallow reservoir with a response delay of 10 days, followed by an inflow of karstic water with a response delay of 70 days, the amount being higher than the saline inflow. Such a process probably results from changes in volumetric strain with subsequent microfracturation transient episodes allowing short inflow of deep salted water in the aquifer. This study demonstrates that groundwater systems in such environments are unstable systems that are highly sensitive to both rainfall inputs and microseismic activity. Impulse responses calculation of F to E_s is shown to be a powerful tool to identify transient anomalies. Similar processing is suggested to be potentially efficient to detect precursors of earthquakes when long time-series (5 years at least) are available in areas with high seismicity.

Key words: Hydrochemical time-series, mixing function, transient anomalies, volumetric strain.

1. Introduction

Earthquakes can trigger or be preceded by various types of geochemical and geophysical transient anomalies, the significance of which is still in debate (Geller,

[1]Observatoire Midi-Pyrénées, LMTG, UMR 5563, 14 Avenue Edouard Belin, 31400, Toulouse, France
[2]BRGM, Orléans, France
[3]Observatoire Midi-Pyrénées, DTP, UMR 5562, 14 Avenue Edouard-Belin, 31400, Toulouse, France

1997; GELLER *et al.*, 1997; SYKES *et al.*, 1999; WYSS, 1997, 2001; BERNARD, 2001). Many hydrological (water temperature and level and stream flow) and geochemical (gas contents or ratios) anomalies have been recognized as related to seismic processes, either as precursors or coseismic signals (KING, 1986; THOMAS, 1988; WAKITA *et al.*, 1988; ROELOFFS, 1988; MOGI *et al.*, 1989; MUIR-WOOD and KING, 1993). Most of these anomalies are interpreted as the result of crustal processes occurring at depth.

However, surficial hydrochemical processes may also occur in the sedimentary pile. Aquifers often result from different groundwater sources which continuously mix in various proportions, and earthquake-related processes may change the relative mixing proportions. Abrupt changes in some ion concentrations in groundwaters have been interpreted as short-term precursory anomalies at weak epicentral distances ($D < 50$ kms) (TSUNOGAI and WAKITA, 1995; NISHIZAWA *et al.*, 1998; TOUTAIN *et al.*, 1997; BELLA *et al.*, 1998; BIAGI *et al.*, 2000; FAVARA *et al.*, 2001; ITALIANO *et al.*, 2001). These anomalies are interpreted as resulting from preseismic strain changes, with subsequent variations of hydraulic head levels and/or infiltration of surface waters. Both processes lead to mixing of geochemically contrasted aquifers, and may both occur as the result of a single strain event (TOUTAIN *et al.*, 1998; Poitrasson *et al.*, 1999).

Mixing of aquifers appears therefore as a key process associated with earthquakes. However, unlike physical anomalies (level, temperature) where a large set of data is available, very few hydrochemical anomalies are published and those available concern mainly isolated events characterized by a single couple earthquake-geochemical anomaly. Therefore, the assessment of systematic relationships for a large set of data at a single site is still lacking, as well as the method to evidence such relationships. Such an assessment requires a long-term recording of both seismic and hydrochemical data within a limited and well constrained area, that is very rarely performed.

In this study we have evidenced that the mixing function F characteristic of aquifer dynamics in mixed sedimentary contexts is a key parameter to constraint coseismic hydrologic effects. With this aim, we performed a three-year hydrochemical monitoring of major elements on springwater from the western Pyrénées, which are characterized by a moderate but recurrent seismicity (RIGO *et al.*, 1997; SOURIAU and PAUCHET, 1998; SOURIAU *et al.*, 2001).

2. Seismotectonic and Geochemical Background

2.1 Seismotectonics and Thermal Springs Distribution in the French Pyrénées

The Pyrenean range results from the convergence of the Iberian and Eurasian plates (CHOUKROUNE, 1992; OLIVET, 1996). The main structural and geological units of the belt are the Mesozoic sedimentary North Pyrenean zone (NPZ), the granitic

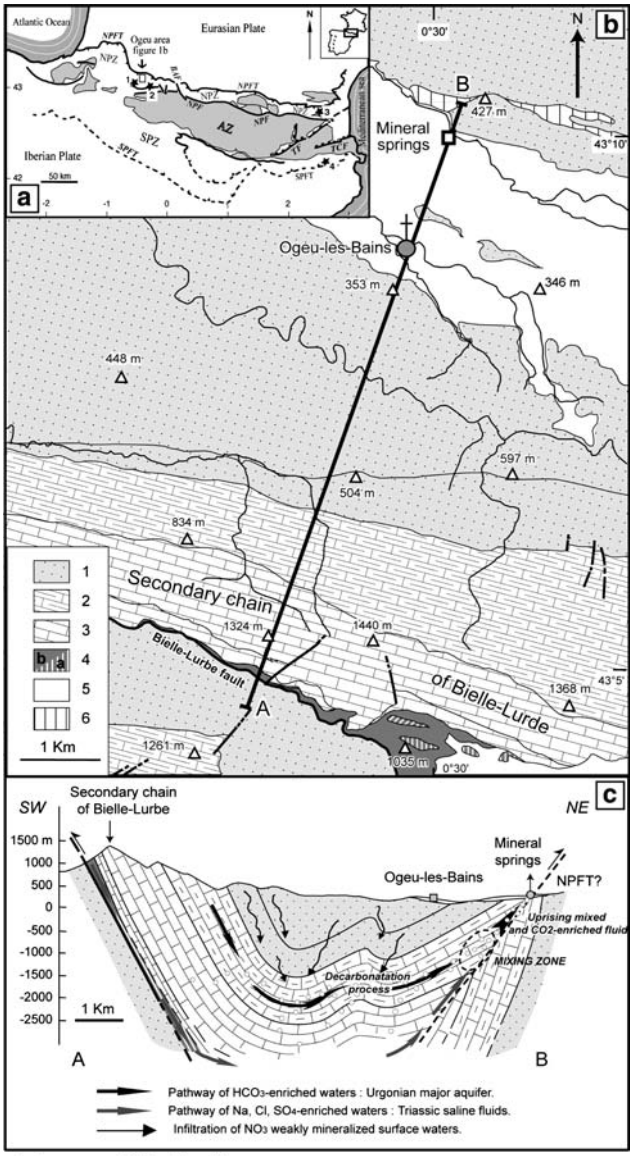

Cretaceous - 1: 'Black flysch'
Jurassic - 2: Urgonian limestones; 3: Limestones and dolomites associated with sandstones and marls.
Trias - 4a: Marls and detritic formations with evaporites (gypsum and halite).
4b: Ophites.
Quaternary - 5: alluviums.
6: Volcanic rocks.

Figure 1

A : Structural sketch map of Pyrénées showing the main faults: NPFT (North Pyrenean Frontal Thrust), BAF (Bigorre-Adour faul), TF (Têt Fault), TCF (Tech Fault) and the main structural domains: NPZ (North Pyrenean Zone), AZ (Axial Zone), SPZ (South Pyreenan Zone). The three main earthquakes of the 20th century are displayed: 1: Arette, M = 5.7, 1981; 2: Arudy, M = 5.6, 1986; 3: St Paul de Fenouillet, M = 5.2, 1996). B: Geological sketch map of the Ogeu area (modified from CASTERAS *et al.*, 1970). C: Interpretative crosssection showing the main structures and potential circulation paths.

and metamorphic axial zone (AZ) and the sedimentary South Pyrenean zone (SPZ), showing an E-W orientation (Fig. 1a), being bounded by three major faults, which are from N to S: the North Pyrenean Frontal Thrust (NPFT), the North Pyrenean Fault (NPF) and the South Pyrenean Frontal Thrust (SPFT). The range displays a permanent, low to moderate seismicity (most of the quakes having magnitudes $M \leq 5$, and three quakes of magnitude > 5 during the last century (Arette, 1967, $M = 5.7$; Arudy, 1980, $M = 5.3$; St Paul-de-Fenouillet, 1996, $M = 5.2$) (SOURIAU and PAUCHET, 1998, Fig. 1a). The distribution of the seismicity is not homogeneous all over the belt: it is concentrated along the NPF west of the Bigorre-Adour fault (BAF), whereas in the central and eastern parts, it is associated with structural features such as granitic bodies, the NPFT and the great fractures relative to the Mediterranean tectonics (Tech and Têt faults).

About 120 mineral waters are identified in the French Pyrénées, mainly distributed along major faults and granitic bodies. Three main chemical patterns can be outlined: 1) alkaline Na-S waters discharge in the AZ, 2) waters with carbonated-evaporitic features (Ca-HCO_3, Ca-SO_4, Na-Cl and intermediate types) rise in the NPZ, and 3) some CO_2-rich springs are recognized along the Tech fault (Na-HCO_3 type) and in the NPZ (Ca-HCO_3 type). Na-S hot waters and CO_2-rich springs of the eastern Pyrénées are well-documented (MICHARD and FOUILLAC, 1980; MICHARD *et al.*, 1980; YERRIAH, 1986; MICHARD, 1990; ALAUX-NEGREL, 1991; KRIMISSA, 1995), but typical Pyrenean carbonate-evaporite waters are still poorly studied (VANARA, 1997). Recently, LEVET *et al.* (2002) investigated water-rock interactions in Pyrenean tectonically active sedimentary terrains and outlined the extend of mixing processes. TOUTAIN *et al.* (1997) and POITRASSON *et al.* (1999) showed in the eastern Pyrénées that such multiple mixing processes vary continuously with time and may be disturbed by seismic processes.

2.2 Hydrogeological Background of the Ogeu Area

The Ogeu area is made of Upper Triassic detrital and evaporitic (anhydrite and halite) deposits covered by less than 3000 meters thick Jurassic and Cretaceous limestone-dolomite formations associated with marl, sandstone and clay layers (CASTERAS *et al.*, 1970; CASTERAS,1971). Quaternary deposits (alluvial formations less than 25 m thickness) are crossed by the uprising of Ogeu waters. BERARD and MAZURIER (2000) identified the Urgonian limestones as the main karstic aquifer feeding all the local springs. The local structure is composed of a synclinal followed by an anticline; the bend of which is straight below the Ogeu-les-Bains discharges (Fig. 1c), probably acting as a drain for underground circulations. 'Black Flysch' mainly composed of slaty limestones and marls fill the depression-shaped valley in the study area (Fig. 1b).

The Bielle-Lurbe secondary chain (Fig. 1) is the local recharge area (BERARD and MAZURIER, 2000). The seepage to depth of meteoric waters is probably fast, through

the subvertical bedding of the Mesozoic layers and a well-developed network of fractures in karstic terrains (CASTERAS *et al.*, 1970).

Three natural springs ('A', 'B', 'H'), three wells ('AEP1', 'AEP2', 'Labourie') and two drillholes ('C', 'Bel Air') rise in the Ogeu area. Mineral waters are of HCO_3-Ca-(Na-Cl) type (Table 1). Temperatures are in the range 21 ± 2°C, pH in the range 5.6–7.7 and TDS in the range 300–848 mg/l. CO_2 degassing occurs at 'A' and 'H' springs and 'Bel Air' drillhole. The lack of CO_2 in C waters may be due to early demixion of the gas owing to the specific geometry of the hydrologic circuit. The 'H' and 'C' waters are bottled for commercialization. We used C water for hydrochemical monitoring.

3. Methods

3.1 Chemical Analyses

326 commercial bottles of C drillhole water have been collected from March, 1997 to June, 2000. Water remained stored in these bottles during a mean period of 1 year prior to processing. TSUNOGAI and WAKITA (1995) and TOUTAIN *et al.* (1997) showed that a two-year storage in similar conditions does not significantly affect major anion and cation concentrations, except limited changes of HCO_3^- resulting from slow degassing. This makes such bottled waters suitable for chemical monitoring.

Waters were filtered at 0,2 μm with an acetate cellulose membrane. Aliquots for major cations were acidified to pH ≤ 2 with ultrapure 14N HNO_3. Ca^{2+}, Mg^{2+}, Na^+ and K^+ were measured by atomic adsorption spectrophotometry. Anions (Cl^-, SO_4^{2-} and NO_3^-) were analyzed by ion chromatography. The international geo-standard SLRS-4 is used to check the accuracy and reproducibility of the cations analyses. Analytical errors are below 4% for all elements, excepting for calcium (< 7%) probably because of interferences. To correct long-term instrumental drifts, a running sample is analyzed with every set of samples. Concentrations of cations and anions are calculated using an external home-made standard. Twenty-five bottled waters distributed over the whole time-series have been analyzed for total alkalinity (HCO_3^-) and SiO_2 concentrations by using Gran's method and molybdate colorimetry, respectively. The mean concentration of HCO_3^- (3.0 meq/l) has been used to calculate the charge mass balance for all the samples. The charge imbalance is less than 8% for all the samples with a mean value of 3%, which can be considered as an acceptable value.

3.2 Equilibrium Calculations

Major elements ratios and saturation indexes (SI = Log Ion Activity Product/formation constant K) are used to highlight water/rock interactions. The SI of pertinent mineral phases with respect to the sedimentary environment (calcite, aragonite, ordered- and disordered-dolomite, anhydrite, halite, chalcedony) have been calculated for outlet conditions with the EQ3/6 software (WOLERY and DAVELER, 1992) and the SUPCRT92 thermodynamic database (JOHNSON *et al.*, 1992).

Table 1

Chemical (mmol/kg) and isotope analyses (‰) of selected waters. Saturation Indexes (SI) are calculated for calcite (calc), aragonite (arag), disordered- (dis-) and ordered-dolomite (ord-), anhydrite (anhy), halite (hali) and chalcedony (chal)

			°C		mmol/kg									meq/l		%		SI						
	Type	Date	T	pH	$H_2CO_3^*$	HCO_3^-	SiO_2	Ca^{2+}	Mg^{2+}	Na^+	K^+	Cl^-	SO_4^{2-}	NO_3^-	Ca + Mg/ HCO_3 + SO_4	Na/ Cl	$\delta^{18}O$	δD	calc.	arag.	dis-	ord-	anhy.	hali.	chal
"C" water																								
C9901	d	25/01/ 1999	23	7,5	–	3,06	0,20	1.06	0.47	1.49	0.02	1.34	0.02	–	0.99	1.1	−6.4	−50.0	−0.1	−0.2	−0.9	0.7	−3.7	−7.4	0.1
Mean (n = 360)	d	–	–	-	–	n.a.	0,21	1.28	0.51	1.47	0.03	1.51	0.18	0.07	1.04	0.97	–	–	−0.02	−0.16	−0.81	0.75	−2.70	−7.31	0.09
Mean (n = 25)	d	–				3,08									1.04										
A.U.(±)		–	–	–	–	0,06	0,004	0.04	0.01	0.03	0.001	0.03	0.004	0.003	–		–	–	–	–	–	–	–	–	–
2s		–	–	–	–	0,15	–	0.08	0.019	0.15	0.003	0.15	0.012	0.015	–		–	–	–	–	–	–	–	–	–
AEP1	w	12/04/ 1994	-	7,6	–	2,87	0.14	1.28	0.35	0.65	0.03	0.73	0.10	0.08	1.06	0.9	–	–	0.0	−0.1	−0.9	0.7	−3.0	−8.0	0.0
AEP2	w	14/09/ 1992	19	7,6	–	2,82	0.08	1.24	0.38	0.87	0.03	0.96	0.13	0.08	1.05	0.9	–	–	0.0	−0.1	−0.9	0.7	−2.9	−7.7	−0.3
A	s	12/01/ 1994	21	7,1	0,14	3,00	0.11	1.23	0.46	1.32	0.04	1.37	0.18	0.05	1.01	1.0	–	–	−0.5	−0.6	−1.8	−0.2	−2.9	−7.3	0.2
B	s	03/12/ 1985	21	7,7	–	3,05	–	1.20	0.50	1.31	0.03	1.29	0.21	0.05	0.98	1.0	–	–	0.1	0.0	−0.6	1.0	−2.7	−7.4	−0.3
H	s	14/05/ 1997	20	5,6	7,66	3,15	0.16	1.25	0.48	1.48	0.02	1.54	0.19	0.05	0.98	1.0	–	–	−2.2	−2.3	−5.2	−3.6	−2.7	−7.3	0.0
Bel Air	d	15/10/ 1986	17,4	7,2	0,43	5,10	0.11	1.90	1.17	0.43	0.02	1.05	0.14	0.02	1.14	0.4	–	–	0.0	−0.2	−1.2	0.4	−2.7	−7.6	−0.1

4. Chemical Composition and Water-rock Interactions

4.1. Chemical composition

Only one isotopic measurement is available ($\delta^{18}O = -6{,}4‰$ and $\delta D = -50‰$, Table 1), which is typical of a meteoric origin with an Atlantic signature. The very weak shift (1‰) with respect to the Global Meteoric Water Line (GMWL; CRAIG, 1963) indicates that no isotopic exchange between rocks and fluids occurs at depth because of low aquifer temperatures.

The chemical composition of Ogeu waters, together with mean concentrations of drillhole 'C' waters are shown in Table 1. The total mineralization ranges from 8 to 13 meq/l. HCO_3^- and $Ca^{2+} + Mg^{2+}$ are the dominant ions indicating a major carbonate contribution. A lower (2 to 4 meq/l, that is to say 22 to 38% of the total mineralization) saline component ($Na^+ + Cl^- + K^+ + SO_4^{2-} + (Ca^{2+} + Mg^{2+} - HCO_3^-)$) indicates a significant evaporitic contribution. This chemistry is typical of water chemistry in complex sedimentary environments (PASTORELLI *et al.*, 1999; LEVET *et al.*, 2002; MINISSALE *et al.*, 2002).

Time-series of cations and anions are displayed in Figure 2. The mean value plus one or two standard deviations (1 or 2σ) are displayed as empirical thresholds above or below which values are often considered as anomalous. Cations and anions vary mainly within their respective 2σ domains during the three years of monitoring. Very few measurements may be considered as anomalous by considering the mean plus two standard deviation threshold. Considering the mean plus one standard deviation should lead to very contrasted results in terms of anomalous/versus non anomalous periods. Moreover, considering alternatively each element should lead to the identification of different anomalous periods. This highlights that assuming an empirical threshold constituted by the mean plus one or two standard deviations is not a reliable method.

Cl^- and SO_4^{2-} ions display seasonal patterns, with higher concentrations in summer (Fig. 2), whereas Ca^{2+}, and Mg^{2+} show no clear seasonal variations. The contribution of chemically different fluids in Ogeu water may explain this different behavior. Morever, Cl^-, SO_4^{2-} and Na^+ likely behave conservatively (and their contents can be affected by dilution/concentration processes) while Ca^{2+} and Mg^{2+} are likely controlled by a mineral phase (Ca-Mg carbonate) either in diluted or concentrated fluids through the seasons.

4.3 Water-rock Interactions

In a carbonate-dominated environment, pCO_2 controls equilibria with respect to carbonate mineral phases (DREYBRODT *et al.*, 1996). "C" is saturated with respect to calcite and aragonite ($SI_{mean} = -0.1$ and -0.2, respectively). The weak oversaturation with respect to ordered-dolomite ($SI_{mean} = 0.7$) likely results from early demixion of CO_2.

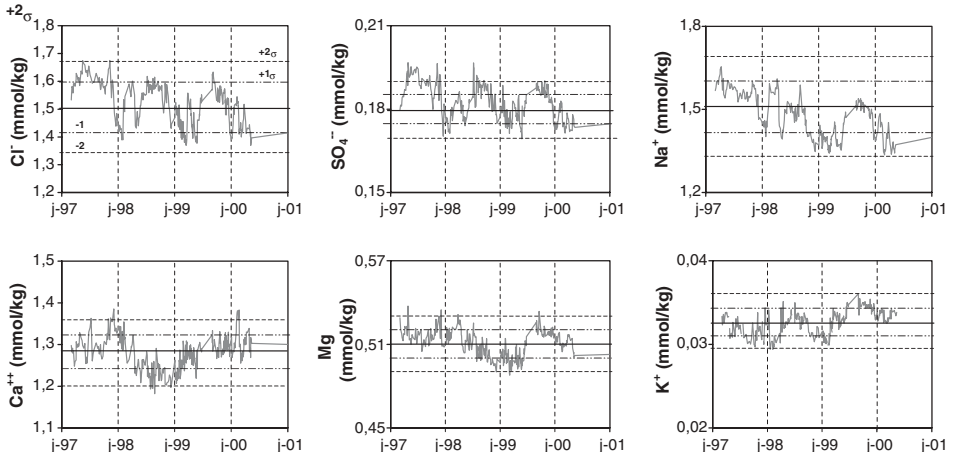

Figure 2
Hydrochemical time-series. Mean and ± 2 sigmas thresholds are displayed.

The calculated $(Ca^{2+} + Mg^{2+})/(HCO_3^- + SO_4^{2-})$ ratios (in meq/l) of the 25 drillhole "C" samples for which alkalinity was measured and for the other emergences vary from 0,98 to 1,14 (Table 1). This suggests that these four ions originate from stoichiometric dissolution of both mixed calcium and magnesium carbonates and sulphates. This confirms Ogeu waters to percolate both Mesozoic carbonates (Urgonian limestones and dolomites) and Triassic rocks (anhydrite- and halite-bearing evaporites).

The Figure 3 displays variations between Cl and Na and SO_4 concentrations (in mmol/kg) for the time-series and the discrete samples. The mean Na/Cl molar ratios of samples from the time-series is 0.97 ± 0.03 (Table 1, Fig. 3a), which confirms that Cl and Na ions originate from stoechiometric dissolution of halite. The linear correlation (σ^2 = 0,80) shown in Figure 2b between sulphate and chlorine concentrations suggests the Triassic evaporitic layers as a common rock source for these two ions. Ogeu waters are strongly undersaturated with respect to halite and anhydrite (SI_{mean} = −7,5 and −2,9 for halite and anhydrite respectively) that could result either from a high water/rock ratio (limited occurrence of halite and anhydrite in Triassic evaporites layers) or a mixing between deep saline fluids and weakly mineralized groundwaters, or probably both. Moreover, as anhydrite displays both a high dissolution rate and retrograde solubility, such a strong undersaturation likely indicates that anhydrite is not present along the upflow pathway. This confirms that Ogeu water results from the mixing of two independant reservoirs: a Urgonian carbonated aquifer and a saline fluid resulting from leaching of Triassic evaporitic layers. According to the local tectonics (Fig. 1c) and to strong anhydrite undersaturation (Table 1), the saline body is deeper than the karstic aquifer. Saline fluids

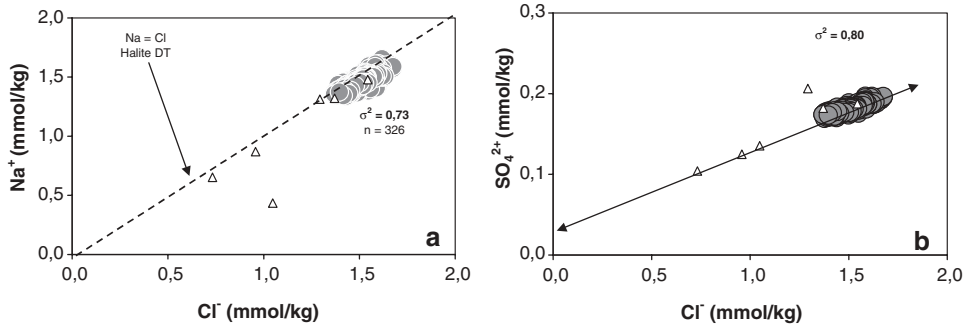

Figure 3
Concentrations of main ions (SO_4^{2-}, Na^+) as a function of chlorine (mmol/kg).

probably migrate along a deep-rooted fracture developed inside the Ogeu's anticlinal, and mixes with the Urgonian water body.

K concentrations are very low (0,02 to 0,04 mmol/kg). In similar sedimentary environments, aqueous potassium commonly originates from interactions (dissolution, ions exchange) with marls and clays interbedded with the dominant limestones and dolomites formations (MARINI *et al.*, 2000; MINISSALE *et al.*, 2000; LEVET *et al.*, 2002). This is confirmed in Ogeu context by the lack of correlation between K and Cl ($\sigma^2 = 0{,}05$), mainly as the result of ions exchange with clays.

In low-temperature hydrothermal systems hosted in carbonate-evaporite bodies, silica has long been suggested to be controlled by poorly crystalline silica phases, most often chalcedony (ARNÓRSSON, 1975; AZAROUAL *et al.*, 1997; PASTORELLI *et al.*, 1999). This is consistent with the chalcedony SI values (−0,29 to 0,15) calculated for all the waters.

4.4 Quantification of the Mixing Process

Because Cl ions are conservative elements and originate from a single saline deep source in Ogeu context, their concentrations are suitable to quantify the mixing process. The chemistry of the two end-members involved in the mixing process for Ogeu waters (carbonated water and saline water) is unknown, but can be approximated by using hydrochemical data from similar geologic environments.

The Bagnères-de-Bigorre thermal waters which rise in the sedimentary NPZ are typically derived from interactions of fluids with Triassic evaporite deposits at depth since they display a mixed Ca-SO_4/NaCl character and an estimated equilibration temperature around 60°C (LEVET *et al.*, 2002). Depending on the relative amounts of choride and sulfate minerals in the Triassic levels, the derived fluids may be Na-Cl or Ca-SO_4 dominated. With a mean composition for dominant elements, $Cl^- = 3.1$, $Na^+ = 3.2$, $Ca^{2+} = 13.6$, $Mg^{2+} = 3.1$ and $SO_4^{2-} = 16.1$ mmol/kg, the Bagnères-de-Bigorre waters can be used as the saline end-member for its chloride character.

The chemistry of Mesozoic west Pyrenean karstic aquifers is characterized by the absence of SO_4^{2-}, very low Cl^- contents and displays mean concentrations of about 2.6, 1.3, 0.2 and 0.05 mmol/kg for HCO_3^-, Ca^{2+}, Cl^- and NO_3^-, respectively (VANARA, 1997) which can be used as the carbonate end-member.

The mixing function F corresponds to the percentage of carbonated water in the mixture. It is calculated with a binary mixing equation based on mass balance and Cl contents, Cl_{mix} being a linear function of F:

$$Cl_{mix} = F(Cl_s - Cl_k) + Cl_k, \tag{1}$$

where Cl_{mix} is the measured concentrations in mmol/kg of 'C' drillhole water, Cl_k is the mean concentration of western Pyrenean karstic waters (0.17 mmol/kg) and Cl_s is the concentration of the deep evaporitic end-member (3.1 mmol/kg).

Results (Fig. 4) show that F varies from 49 to 60% within the 2σ interval over the time-series. The absolute values of F obviously depend on the respective concentrations of both saline and carbonate end-members. The mixing function F appears therefore as a good tracer of the dynamics of the Ogeu aquifer.

5. Rainfall and Seismic Time-Series

Surficial karstic aquifers are usually complex hydrological and hydrochemical systems opened to various fluid circulations and therefore may be strongly influenced by rainfall and permanent crustal stresses. Seasonal recharge, particular rainfall events and continuous crustal stress changes may therefore contribute to the control of the chemical composition of the water. In sedimentary areas, strain build-up

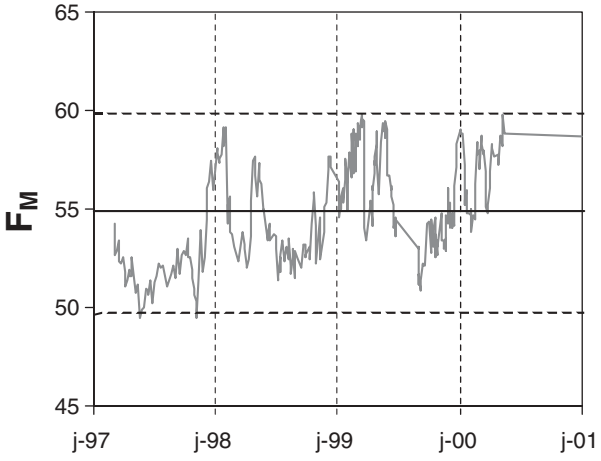

Figure 4
Time-series of the calculated mixing function F. Mean and ± 2 sigmas thresholds are displayed.

induced by major earthquake preparation process is often suggested to account for the mixing of waters of contrasted chemistry (THOMAS, 1988; WAKITA *et al.*, 1988; TSUNOGAI and WAKITA, 1995; TOUTAIN *et al.*, 1997). Such a basic assumption, however, should be considered together with the dynamic response of the aquifer to current external perturbations, due to rainfall recharge and background seismicity. It is to be noted that up to now, papers dealing with geochemical anomalies related to severe seismic events never took into account such perturbations. In this section, time-series for rainfall, seismic activity and chemical composition of the waters are displayed for a three-year period.

5.1. Rainfall Time-series

Monthly rainfall data recorded from March 1997 to May 2000 at 20 km distance from Ogeu are shown in Figure 5. No clear periodicity of rainfall can be distinguished, probably as the result of both a strong oceanic character and multiple minor climatic influences. However, some periods of heavy rainfall can be identified and may constitute events that potentially trigger impulse responses from the aquifers.

5.2 Seismic Time-series: Energy Released and Epicentral Distributions

The area under consideration is monitored by a homogeneous array of seismological stations from the Observatoire Midi-Pyrénées; five of which lie within 50 km of the spring location (SOURIAU *et al.*, 2001). During the period March 1997

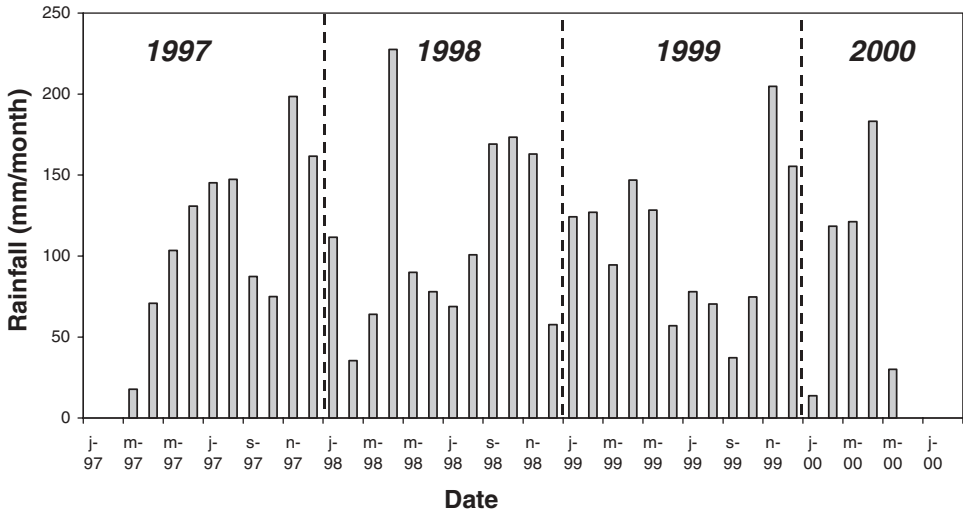

Figure 5
Rainfall time-series. Daily measurements are performed 20 km south of the Ogeu seismic station. Monthly mean variations are displayed.

to June 2000, 448 earthquakes were recorded and accurately located within 30 km distance of the spring, with magnitudes spanning the range 0.3–4.0. 55 of these events, with 0.3 to 3.6 magnitudes, were located closer than 10 km from the spring (Fig. 6). Most of the earthquakes were situated south of the spring, on the north-dipping NPF. Their depths (in the 10-km radius circle) extend from 0 to 16 km, with an average value of about 8 km. The average horizontal and vertical errors on the epicenters are of the order of 1.5 and 3.0 km.

In order to characterize the influence of seismic events on the mixing function, the key parameter is the seismic energy E_S radiated by the earthquakes. This parameter can be connected to the magnitude through empirical laws. Care has to be taken in

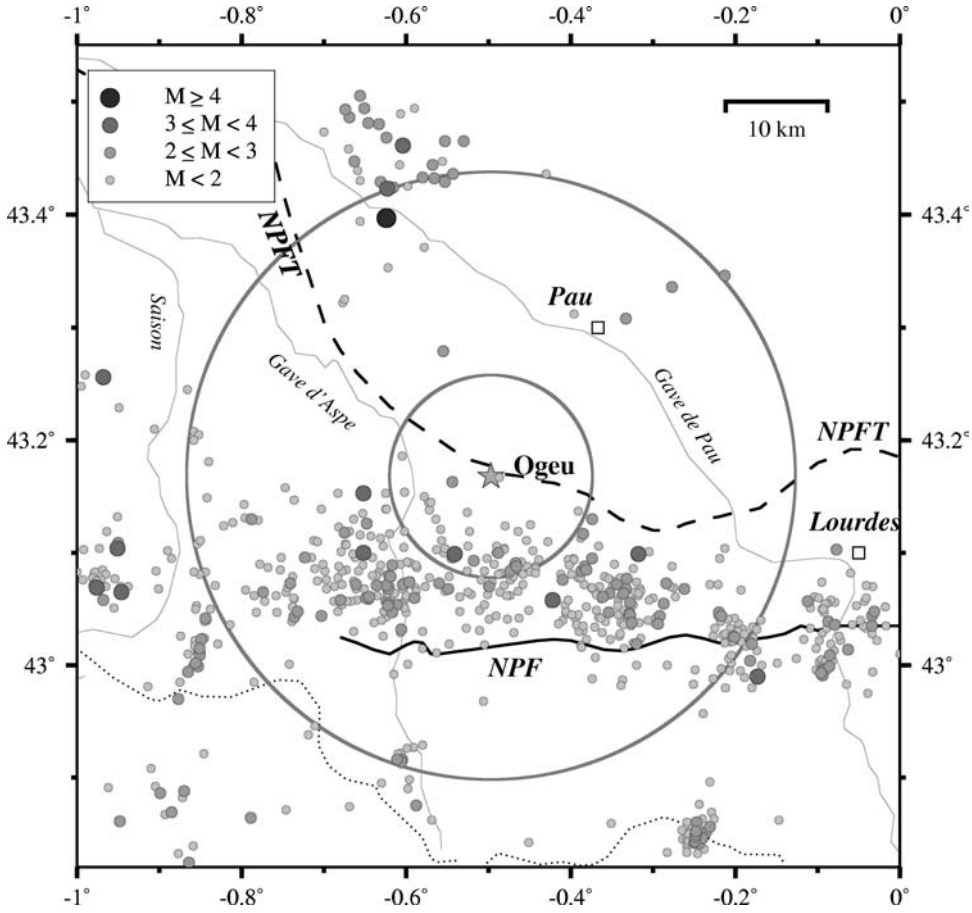

Figure 6
Epicentral map of seimicity in the Ogeu area for the period March 1997 – June 2000. The size of the symbols increases with earthquake magnitude. The star indicates the spring location. Circles with radii 10 km and 30 km centered on the spring are displayed. NPFT : North Pyrenean Frontal Thrust; NPF: North Pyrenean Fault.

the choice of these laws, since they closely depend on the kind of magnitude scale under consideration. In the earthquake catalogue used, the magnitudes of the events are local (or Richter) magnitudes M_L. For this particular kind of magnitude, KANAMORI *et al.* (1993) obtained a very simple linear relationship $\log_{10}(E_S) = 1.96\ M_L + 9.05$, where the energy E_S is in ergs.

Figure 7 shows the amount of seismic energy radiated during the considered period in the 30 km and 10 km radius circular areas centered on the spring. Events were grouped within time windows of 10 days. The values displayed are lower bound estimates, since the seismological array can fail in the detection of minor events (with magnitudes smaller than about 1.5). However, owing to the exponential dependence of energy on magnitude, the total budget is not greatly affected by the loss of small earthquakes. These plots illustrate well the fact that the seismic activity is not

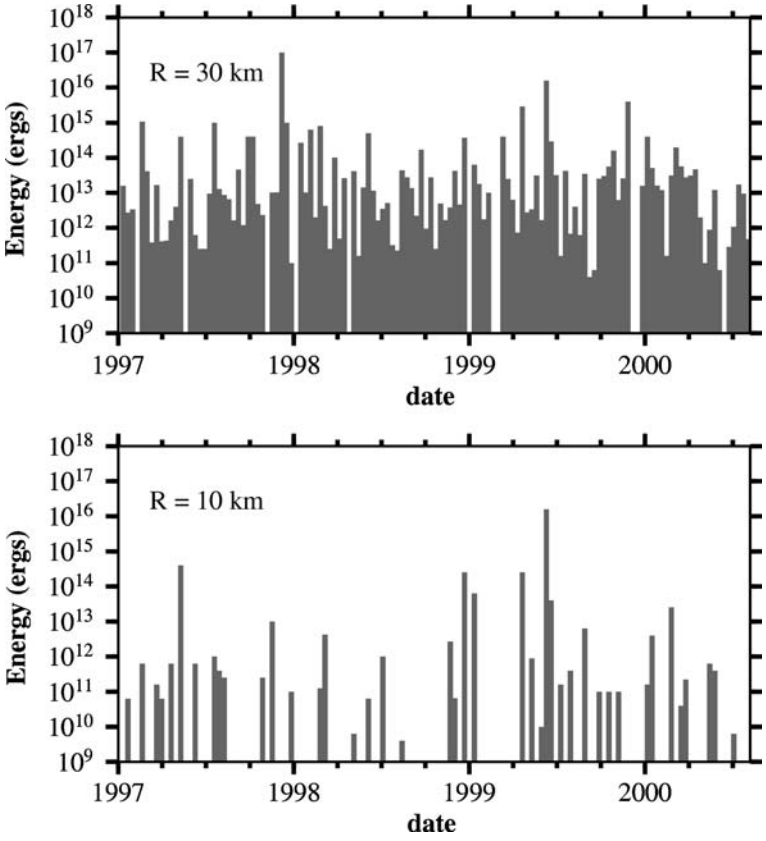

Figure 7
Seismic energy release in a 30 km radius (upper plot) and 10 km radius (lower plot) circular area around the Ogeu sampling site, within 10-day time windows.

continuous, and periods with higher-than-average rates of energy released can be identified, in particular during the year 1999.

6. The Mixing Function Versus the Energy of Earthquakes and Effective Rainfall

The purpose of this paragraph is the study of the response of the mixing function F according to both energy E_S of earthquakes whose distance of epicenter to the monitoring site is nearer than 10 kilometers and the effective rainfall R at Ogeu. Variations of the mixing function F represent the amount of fresh carbonated water into the shallow reservoir.

The energy function M is calculated as $\log_{10}(E_S)$ where E_S is the seismic energy of events grouped within 10-day time windows.

The mixing function F can be represented as a linear relationship of M and R such that

$$F = \Gamma_M * M + \Gamma_R * R + C^{st}, \tag{1}$$

where Γ_M and Γ_R are the impulse responses of F to the magnitude M and to the effective rainfall R, respectively; $f * g$ represents the discrete convolution product between time series f and g:

$$[f * g](j) = \sum_{i=0,N} f_i \cdot g_{j-i} = \sum_{i=0,N} f_{j-i} \cdot g_i, \tag{2}$$

N is the order of impulse response f or g.

The calculation of Γ_M, Γ_R and the constant C^{st} from the time series F, M and R uses a regularization method since the inversion of equation (1) is an ill-posed problem. Indeed, an infinity of solutions may fulfill equation (1) and the more likely solution is selected so that its norm is minimum in order to make Γ_M and Γ_R as smooth as possible (PINAULT *et al.*, 2001).

A constant C^{st} is introduced in equation (1) since only the variations of the mixing function F are to be explained from M and R so that:

$$\Delta F = \Gamma_M * \Delta M + \Gamma_R * \Delta R, \tag{3}$$

where $\Delta F = F - \bar{F}$, $\Delta M = M - \bar{M}$ and $\Delta R = R - \bar{R}$, $\bar{F}$, $\bar{M}$ and $\bar{R}$ being the mean of F, M and R.

Equation (2) represents the more general linear relationship between inputs and an output. It is characterized by impulse responses, i.e., the response of the output when inputs are impulses (they last exactly one sampling step, i.e., 10 days). In the present case the inputs are effective rainfall R and the magnitude M. Impulse responses represent the response of the mixing function F after a hypothetical isolated event (a rainfall event or a seismic event depending upon the impulse response). Once the impulse responses are known, the two terms of the second

member of equation (3) represent the contribution of both inputs (rainfall and magnitude) to the mixing function F.

Impulse response Γ_M of the mixing function F to the energy function M is equivalent to the variation of F subsequent to a quake for which $M = \log_{10}(E_S)$, i.e., an event of magnitude $M_L = (M - 9.05) / 1.96$. In such a model, the perturbation of F is proportional to the magnitude.

In the same way, impulse response Γ_R of the mixing function F to the effective rainfall R represents the variation of F subsequent to a rainfall event whose height is R and, here again, the perturbation of F is proportional to the height of the effective rainfall event.

Resolution of equation (1) is performed with a 10 day sampling rate. Figure 8 shows the output of the mixing function F versus both inputs M and R. Figure 9(1) exhibits the comparison between the model (equation 2) and the mixing function F. Discrepancies arise during the first year due to the truncation of time series M and R in equation (1): the length of impulse responses is therefore 250 days. Figure 9(2) shows the comparison between the model (equation 1) and the mixing function F when only effective rainfall R is used as input. Discrepancies between the model and F increase significantly between (1) and (2), evidencing the relevancy of the energy M used as input in the model.

The time series representing both inputs and the output are centered in order to remove the constant in equation (2). The calculation of the two impulse responses requires the use of a regularization technique since, as a mathematical point of view, it is an ill-posed problem (many solutions can fulfill the requirements). The regularization technique consists in selecting the 'smoother' solution while the discrepancies between the observed mixing function F and the model are minimal. To accomplish that the Tikhonov regularization technique is used (TIKHONOV and GONCHARSKY, 1987). The solutions that are obtained from this regularization technique are the more realistic according to the parsimony principle, which tries to explain a phenomenon from the minimum number of arbitrary parameters. Moreover, this technique minimizes the error propagation since the norm of the impulse responses is minimal.

Figure 10 (1) shows impulse responses of F to M (Γ_M) and $R(\Gamma_R)$. Impulse response of F to R represents the recharge of the shallow reservoir due to an increase in pressure head after a rainfall event. It increases drastically after a rainfall event, reaching its maximum 10 days after the event and then decreases for 150 days.

Impulse response of F to M may exhibit the intrusion of salted water into the shallow reservoir after a quake that exerts a constraint on the deep feeding system. It decreases very rapidly after a quake, owing to the increase of chloride concentration into the shallow reservoir. This burst is very short since the impulse response increases 30 days after the quake, when fresh-carbonated water replaces salted water, and reaches a maximum 70 days after the quake. The amount of fresh-carbonated water introduced after the quake is higher than the amount of salted water it is

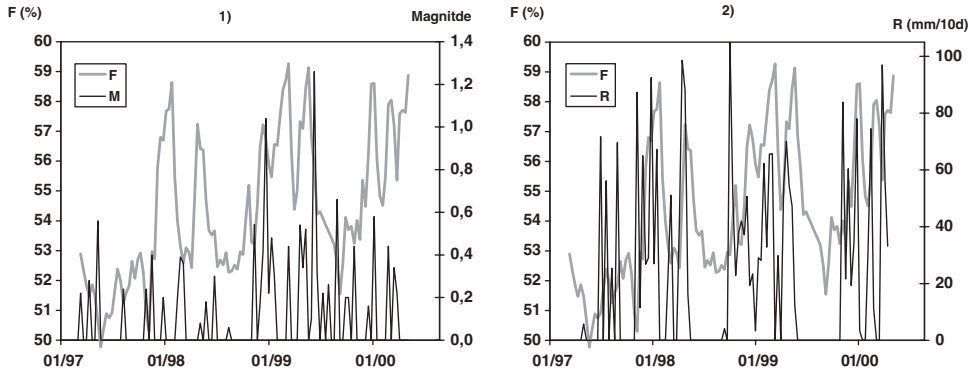

Figure 8
Direct correlation between F (mixing function) and M (energy of events at epicentral distances < 10 km) and between F and R (effective rainfall).

assumed to replace, as shown in Figure 10 (2) that displays the two components of F related to M and R, namely $\Gamma_M * M$ and $\Gamma_R * R$. The response of F to earthquakes manifests therefore long-term variations and it increases in 1999, due to the high magnitude of earthquakes. The deep reservoir behaves as if the compression that occurs during the quake was followed by decompression a few ten-day periods after the quake. The impulse response of F to M becomes inaccurate when the lag overreaches 100 days because of the shortness of time series in comparison to the length of impulse responses, which makes its interpretation hazardous beyond this lag. Correspondingly, the impulse response is too noised to be interpreted at negative lags to bring to the fore precursor signals.

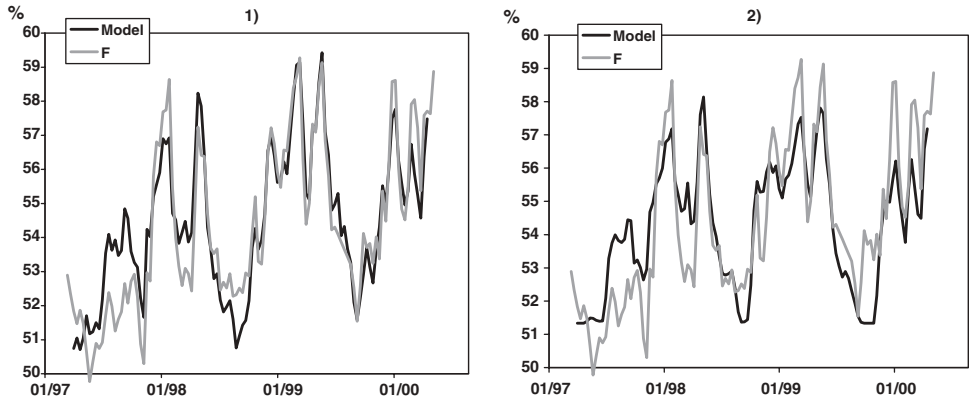

Figure 9
Comparison of the mixing function F and the model with R and M as inputs (equation 1). 2: Comparison of the mixing function F and the model with only R (rainfall) as input.

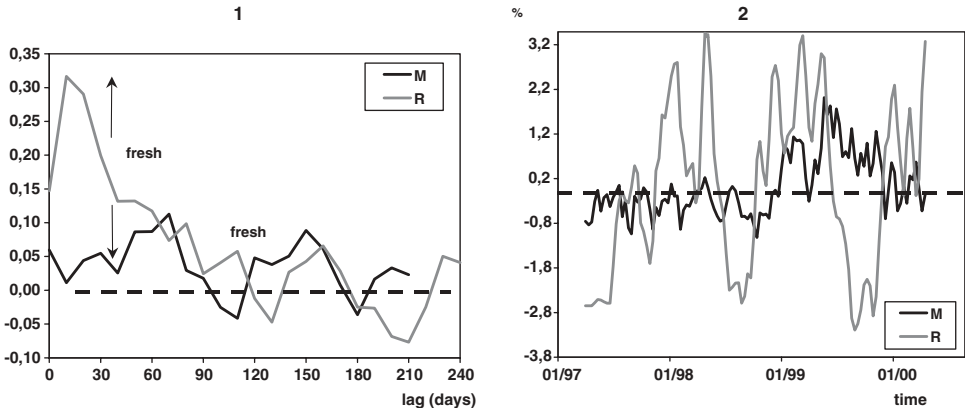

Figure 10
1) Impulse responses of F to M and R. 2) Response of F to earthquakes (M) and rainfall (R).

7. Discussion

Limitations of using arbitrary thresholds. Bulk chemical time-series display variations for which interpretations vary strongly when using either the mean + 1σ or 2σ thresholds, or when considering one or another element. Even if this common practice may be convenient, our results evidence that in many case it is not suitable to detect transient anomalies, at least when the signal/background ratio is limited. Further evidence exists that local water-rock interactions are key constrains for selecting chemical tracers because elements may be controlled either by superficial interactions (e.g., K^+ through ions exchange with clays) or by dissolution/precipitation reactions (e.g., Ca^{++} controlled by carbonates precipitation resulting from CO_2 degassing). Calculation of Saturation Index and observation of the behavior of elements with respect to conservative elements (mainly Cl) have therefore to be performed prior to selecting elements for geochemical survey.

Methodology. Our results confirm that groundwater in mixed carbonated/evaporitic environments is the result of complex interactions between chemically contrasted reservoirs. Mixing processes are the most likely to occur and can be described as discontinuous and fast processes which appear to be controlled mainly by rainfall inputs when strain is assumed to be constant. TOUTAIN *et al*. (1997) and POITRASSON *et al*. (1999) evidenced that multiple mixing processes can affect karstic-dominated groundwater under strain built-up. LEVET *et al*. (2002) demonstrated that using a simple binary mixing equation based on mass balance and Cl^- contents enabled to the calculation of mixing proportions between the two main poles (deep saline and surficial carbonated poles). Considering the temporal fluctuations of the mixing function F may therefore supply information pertinent to crustal processes linked to earthquake preparation and/or triggering. Figure 9(1) evidences that in the sedimentary Ogeu area, which undergoes both discontinuous rainfall recharge and

seismic activity, the mixing function F is the result of both inputs. The involvement of earthquakes in F is confirmed by Figure 9(2), which demonstrates that F cannot be the result of only rainfall inputs. In the Ogeu context, because chlorine concentrations in the fresh-karstic end-member are close to zero, the mixing function is very similar to the 1/Cl concentration of the total fluid. In other contexts, F may be calculated by using any other method based on major or trace elements as well as isotopic ratios.

Crustal processes. As expected, impulse response of F to R constitutes an increase of the contribution of fresh-carbonated water in the discharge. The delay of response in Ogeu conditions is immediate (10 days with a 10-day sampling resolution). On the contrary, the impulse response of F to M is a two-step process with step 1 being a decrease of F, which corresponds to an increase of the contribution of salted water into the shallow reservoir, followed by step 2 that is an increase of F which results from either a decrease of the salted content or an increase of the carbonated contribution. The two-phase process shows response delays of 10 and 70 days for steps 1 and 2, respectively. It is to be noted that the increase of F during step 2 is higher than its decrease during step 1. In other words, the inflow of fresh-carbonated water (step 2) in the reservoir is higher than the inflow of salted water (step 1). This may suggest that step 2 can be due to an inflow of fresh-carbonated water rather than the decrease of salted contribution. Another hypothesis is a simple relaxation process during which normal conditions are reached.

Few crustal processes can be evokated to interpret these observations. The most immediate is the crustal stress variation and/or migration following the earthquakes and allowing the inflow of deeper salted water. Nevertheless, considering the small magnitudes, the epicentral distances and the depths of the seismic events, it is difficult to invoke this phenomenon alone. Preseismic fluid overpressures and variations of the permeability in the fault zones inducing fluid migrations are closely established for earthquakes with magnitude greater than 5 (e.g., MUIR-WOOD and KING, 1993; SIBSON, 1994; HUSEN and KISSLING, 2001; YECHIELI and BEIN, 2002). These fluid migrations highly dependent on the earthquake mechanism are invoked to explain the poro-elastic postseismic deformation (PELTZER *et al.*, 1998) and the triggering of aftershock sequences and the migration of seismic ruptures (NOIR *et al.*, 1997). Regarding micro-seismicity, the focal mechanisms, and therefore, the deformation features are mostly unknown in detail. Consequently, small events frequently distributed in clusters must be considered as volumetric deformation. For example, KOIZUMI *et al.* (1999) showed that earthquake swarms with magnitude of two could be responsible for groundwater level variations in instrumented boreholes associated with changes in volumetric strain. In our Pyrenean case, the two-step feature of the impulse response of F should be associated with the volumetric strain variations linked to the seismic activity. This deformation induced by or inducing micro-seismicity, may allow the opening of microfractures and, then, the inflow of deeper salted water (YECHIELI and BEIN, 2002). Then, the opened fractures may be closed

several days later if no other seismic event occurred. Unfortunately, the 10-day resolution of our results does not allow us (i) to ascertain if the inflow salted water is a response of a seismic event (co- and postseismic response) as we hypothesize in our model, or if it is a preseismic response as described by KOIZUMI *et al.* (1999), and (ii) if the hypothesis of a linear response of the groundwater to an event is reasonable. Nevertheless, it is unquestionable that our observations cannot be explained without considering the moderate, but continuous, regional seismic activity.

8. Conclusion

Thermo-mineral waters rising in sedimentary environments such as Ogeu often result from the mixing of chemically contrasted end-members. Temporal fluctuations of the fluid chemistry can be described by using a mixing function (F), which is calculated by using Cl^- contents in the Ogeu case. However, various parameters (isotopic ratios, trace elements concentrations, elemental ratios, …) may be used to constrain and to calculate the mixing function F according to hydrogeological contexts.

Modelling F over a 3.5-year period by using E_s (seismic energy release in a 10 km radius) and R (effective rainfall) as inputs evidence the involvement of both phenomena in the temporal fluctuations of F. This is the first time that microseismic activity is shown to contribute to the control of the chemistry of water over an extended period. Impulse response of F to E_s, which is calculated with a 10-day sampling rate, indicates volumetric strain episodes leading to successive and transient migration phases of deep saline fluids in the aquifer.

Such modelling confirms that seismically induced fluid transfers can occur episodically and systematically in a given area. Moreover, this modelling appears suitable to precisely assess the role of various parameters such as hypocentral depths, epicentral distances, and earthquake magnitude on the fluid transfers. Unfortunately, such data processing appears unrealistic in this study as the result of the overly short monitoring period (3.5 years) and the exceedingly moderate earthquake activity. However, it is possible and highly desirable to process altogether hydrochemical and seismic time series already available in areas with strong seismic activity.

REFERENCES

ALAUX-NEGREL, G. (1991), *Etude de l'évolution des eaux profondes en milieux granitiques et assimilés. Comportement des éléments traces*. Ph.D. Thesis. University of Paris VII, 216 pp.

ARNÓRSSON, S. (1975), *Application of the silica geothermometer in low temperature hydrothermal areas in Iceland*, Am. J. Sci. *275*, 763–784.

AZAROUAL, M., FOUILLAC, C., and MATRAY, J.M. (1997), *Solubility of silica polymorphs in electrolyte solutions, II. Activity of aqueous silica and solid silica polymorphs in deep solutions from the sedimentary Paris basin*, Chem. Geol. *140*, 167–179.

BELLA, F., BIAGI, P.F., CAPUTO, M., COZZI, E., DELLA MONICA, G., ERMINI, A., GORDEEZ, E.I., KHATKEVICH, Y.M., MARTINELLI, G., PLASTINO, W., SCANDONE, R., SGRIGNA, V., and ZILPIMIANI, D. (1998), *Hydrogeochemical anomalies in Kamchatka (Russia)*, Phys. Chem. Earth. *23*(9–10), 921–925.

BERARD, P. and MAZURIER, C. (2000), *Ressources en eaux thermales et minérales des stations du département des Pyrénées-Atlantiques. Usine d'embouteillage d'Ogeu-les-Bains*, Rapport BRGM/RP 50174-FR, 43 pp.

BERNARD, P. (2001), *From the search of 'precursors' to the research on 'crustal transients'*, Tectonophysics *338*, 225–232.

BIAGI, P.F., ERMINI, A., KINGSLEY, S.P., KHATKEVICH, Y.M., and GORDEEV, E.I. (2000), *Possible precursors in groundwater ions and gases content in Kamchatka (Russia)*, Phys. Chem. Earth. *25* (3), 295–305.

CASTERAS, M., *Notice Explicative de la Carte Géologique d'Oloron-Ste-Marie (1/50000)*, 2d edition (BRGM, France 1971) *19* pp.

CASTERAS, M., CANÉROT, J., PARIS, J.P., TISIN, D., AZAMBRE, M., and ALIMEN, H., *Carte géologique d'Oloron-Ste-Marie (1/50000)* (BRGM, France 1970).

CHOUKROUNE, P. (1992), *Tectonic evolution of the Pyrénées*, Annu. Rev. Earth Planet. Sci. *20*, 143–158.

CRAIG, H. (1963), *Isotopic variations in meteoric waters*, Science *123*, 1702–1703.

DREYBODT, W., LAUCKNER, J., LIU, Z., SVENSSON, U., and BUHMANN, B. (1996), *The kinetics of reaction* $CO_2 + H_2O = H^+ + HCO_3^-$ *as one of the rate limiting steps for the dissolution of calcite in the system* H_2O-CO_2-$CaCO_3$, Geochim. Cosmochim. Acta. *60* (18), 3375–3381.

FAVARA, R., ITALIANO, F., and MARTINELLI, G. (2001), *Earthquake-induced chemical changes in the thermal waters of the Umbria region during the 1997–1998 seismic swarm*, Terra Nova *13*, 227–233.

GELLER, R.J. (1997), *Earthquake prediction: A critical review*, Geophys. J. Int. *131*, 425–450.

GELLER, R.J., JACKSON, D.D., KAGAN, Y.Y., and MULARGIA, F. (1997), *Earthquakes cannot be predicted.* Science *275*, 1616–1617.

HUSEN, S. and KISSLING, E. (2001), *Postseismic fluid flow after the large subduction earthquake of Antofagasta, Chile*, Geology *29*, 847–850.

ITALIANO, F., MARTELLI, M., MARTINELLI, G., NUCCIO, P.M., and PATERNOSTER, M. (2001), *Significance of earthquake-related anomalies in fluids of Val d'Agri (southern Italy)*, Terra Nova *13*, 249–257.

JOHNSON, J.W., OELKERS, E., and HELGELSON, J.W. (1992), SUPCRIT92: *A software package for calculating the standard molal thermodynamic properties of minerals, gases, aqueous species and reactions from 1 to 5000 bars and 0 to 1000*°C, Computer Geosci. *18*, 899–947.

KANAMORI, H., MORI, J., HAUKSSON, E., HEATON, Th.H., HUTTON, L.K., and JONES, L.M. (1993), *Determination of earthquake energy release and* M_L *using TERRASCOPE*, Bull. Seismol. Soc. Am. *83*(2), 330–346.

KING, C.Y. (1986), *Gas geochemistry applied to earthquake prediction. An overview*, J. Geophys. Res. *91* (B12), 12269–12281.

KING, C.Y., KOIZUMI, N., and KITAGAWA, Y. (1995), *Hydrochemical anomalies and the 1995 Kobe earthquake*, Science *269*, 38–39.

KOIZUMI, N., TSUKUDA, E., KAMIGAICHI, O., MATSUMOTO, N., TAKAHASHI, M., and SATO, T. (1999), *Preseismic changes in groundwater level and volumetric strain associated with earthquake swarms off the east coast of the Izu Peninsula, Japan*, Geophys. Res. Lett. *26*, 3509–3512.

KRIMISSA, M. (1995), *Application des méthodes isotopiques à l'étude des eaux thermales en milieu granitique (Pyrénées, France)*, Ph.D. Thesis, University d'Orsay, Paris XI, 273 pp.

LEVET, S., TOUTAIN, J.P., MUNOZ, M., NEGREL, P., JENDRZEJEWSKI, N., AGRINIER, P., and SORTINO, F. (2002), *Geochemistry of the Bagnères-de-Bigorre thermal waters from the North Pyrenean Zone (France)*, Geofluids *2*, 25–40.

MARINI, L., BONARIA, V., GUIDI, M., HUNZIKER, J.C., OTTONELLE, G., and VETUSCHI ZUCCOLINI, M. (2000), *Fluid geochemistry of the Acqui Terme-Visone geothermal area (Piemonte, Italy)*, Appl. Geochem. *15*, 917–935.

MICHARD, G. and FOUILLAC, C. *Contrôle de la composition chimique des eaux sulfurées sodiques du Sud de la France*. In *Géochimie des interactions entre les eaux, les minéraux et les roches* (eds. Tardy) (Tarbes, France 1980) pp. 147–166.

MICHARD, G., FOUILLAC, C., OUZOUNIAN, G., BOULÈGUE, J., and DEMUYNCK, M., *Geothermal applications of the geochemical study of hot springs in eastern Pyrénées*. In *Advances in European Geothermal Research. Proceeding of the second Internal Seminary. On the results of the EC Geothermal Energy Research* (eds. Strub and Ungemach) (Strasbourg, France 1980), pp. 387–395.

MICHARD, G. (1990), *Behaviour of the major elements and some trace elements (Li, Rb, Cs, Sr, Fe, Mn, W, F) in deep hot waters from granitic areas*, Chem. Geol. *89*, 117–134.

MINISSALE, A., MAGRO, G., MARTINELLI, G., VASELLI, O., and TASSI, G.F. (2000), *Fluid geochemical transect in the Northern Apennines (central-northern Italy): Fluid genesis and migration and tectonic implications*, Tectonophysics *319*, 199–222.

MINISSALE, A., VASELLI, O., TASSI, F., MAGRO, G., and GRECHI, G.P. (2002), *Fluid mixing in carbonate aquifers near Rapolano (central Italy): Chemical and isotopic constraints*, Appl. Geochem. *17*, 1329–1342.

MOGI, K., MOCHIZUKI, H., and KUROKAWA, Y. (1989), *Temperature changes in an artesian spring at Usami in the Izu peninsula (Japan) and their relation to earthquakes*, Tectonophysics *159*, 95–108.

MUIR-WOOD, R. and KING, G.C.P. (1993), *Hydrological signatures of earthquake strain*, J. Geophys. Res. *98* (B12), 22035–22068.

NISHIZAWA, S., IGARASHI, G., SANO, Y., SHOTO, E., TASAKA, S., and SASAKI, Y. (1998), *Radon, Cl^- and SO_4^{2-} anomalies in hot spring water associated with the 1995 earthquake swarm of the east coast of the Izu peninsula, central Japon*, Appl. Geochem. *13*, 89–94.

NOIR, J., JACQUES, E., BÉKRI, S., ADLER, P.M., TAPPONNIER, P., and KING, G.C.P. (1997), *Fluid flow triggered migration of events in the 1989 Dobi earthquake sequence of Central Afar*, Geophys. Res. Lett. *24*, 2335–2338.

OLIVET, J.L. (1996), *La cinématique de la plaque Ibérique*, Bull. Centres Rech. Explor. Prod. Elf Aquitaine *20* (1), 131–195.

PASTORELLI, S., MARINI, L., and HUNZIKER, J.C. (1999), *Water chemistry and isotope composition of the Acquarossa thermal system, Ticino, Switzerland*, Geothermics *28*, 75–93.

PELTZER, G., ROSEN, P., and ROGEZ, F. (1998), *Poroelastic rebound along the Landers 1992 earthquake surface rupture*, J. Geophys. Res. *103*(30),131–30,145.

PINAULT J-L., PAUWELS, H., and CANN, Ch. (2001), *Inverse modeling of the hydrological and the hydrochemical behavior of hydrosystems: Application to nitrate transport and denitrification*, Water Res. Res. *37* (8), 2179–2190.

POITRASSON, F., DUNDAS, S.H., TOUTAIN, J.P., MUNOZ, M., and RIGO, A., (1999), *Earthquake-related elemental and isotopic lead anomaly in a springwater*, Earth. Planet. Sci. Lett. *169*, 269–276.

RIGO, A., PAUCHET, H., SOURIAU, A., GRÉSILLAUD, A., NICOLAS, M., OLIVERA, C., and FIGUERAS, S., (1997), *The February 1996 earthquake sequence in the eastern Pyrénées: Fisrt results*, J. Seismol. *1*, 3–14.

ROELOFFS, E. (1988), *Hydrologic precursors to earthquakes: A review*, Pure Appl. Geophys. *126*, 177–209.

SIBSON, R.H. (1994), *Crustal stress, faulting and fluid flow*. In *Geofluids: Origin, Migration and Evolution of Fluids in Sedimentary Basins*, Geolog. Soc. Special Pub. *78*, 68–84.

SOURIAU, A. and PAUCHET, H. (1998), *A new synthesis of Pyrenean seismicity and its tectonic implications*, Tectonophysics *290*, 221–244.

SOURIAU, A., SYLVANDER, M., RIGO, A., DOUCHAIN, J.M., and PONSOLLES, C. (2001), *Pyrenean tectonics: Mean seismological constraints*, Bull. Soc. Geol. France. *172* (1), 25–39.

SYKES, L.R., SHAW, B.E., and SCHOLZ, C.H. (1999), *Rethinking earthquake prediction*, Pure Appl. Geophys. *155*, 207–232.

THOMAS, D. (1988), *Geochemical precursors to seismic activity*, Pure Appl. Geophys. *126*, 241–266.

TIKHONOV, A.N. and GONCHARSKY, A.V. (Eds.), *Ill-Posed Problems in the Natural Sciences* (MIR, Moscow, 1987).

TOUTAIN, J.P., MUNOZ, M., POITRASSON, F., and LIENARD, A.C. (1997), *Springwater chloride ion anomaly prior to a ML = 5.2 Pyrenean earthquake*, Earth. Planet. Sci. Lett. *149*, 113–119.

TSUNOGAI, U. and WAKITA, H. (1995), *Precursory chemical changes in groundwater: Kobe earthquake, Japan*, Science *269*, 61–63.

VANARA, N., *Dissolution et spéléogenèse en contexte tectonique actif: Le Massif des Arbailles (Pyrenees-Atlantiques, F)*. In *Proceeding on the 6th Conference on Limestone Hydrology and Fissured Media*. (Ed. Jeannin P.Y.) (La Chaux de Fonds, Switzerland 1997), *vol. 2*, pp. 115–118.

WAKITA, H., NAKAMURA, Y., and SANO, Y., (1988), *Short-term and intermediate-term geochemical precursors*, Pure Appl. Geophys. *126*, 267–278.

WOLERY, T. and DAVELER, S.A. (1992), *EQ3/6, A Software Package for Geochemical modelling of Aqueous Systems*, *UCRL-MA-110772 PT IV*. *Lawrence Livermore National Laboratory,* Livermore.

WYSS, M. (1997), *Cannot earthquakes be predicted* ? Science *278*, 487.

WYSS, M. (2001), *Why is earthquake prediction research not progressing faster*? Tectonophysics *338*, 217–223.

YECHIELI, Y. and BEIN, A. (2002), *Response of groundwater systems in the Dead Sea Rift Valley to the Nuweiba earthquake: Changes in head, water chemistry and near-surface effects*, J. Geophys. Res. *107*, 2332, doi:10.1029/2001JB001100.

YERRIAH, J. (1986), *Le thermominéralisme carbo-gazeux du Sud-Est de la France (domaine sédimentaire) dans son contexte sismotectonique*, Ph.D. Thesis. University of Montpellier II, France, 108 pp.

(Received: July 25, 2003; revised: November 22, 2005; accepted: November 24, 2005)